Pages: 14-25/ Vol. 15/ No. 1 /Winter- Spring 2022

Journal of Aerospace Science and Technology

www:jast.ias.ir

Scienctifie-Research Article

Designing the Nonlinear Guidance Law Adaptable to Initial Deviations for the Vertical Landing of the Booster

Morteza Sharafi[1], Nasser Rahbar[2]*, Ali Moharrampour[3], Abdorreza Kashaninia[4]

1-2-3-4 Faculty of Electrical & Computer Engineering, Malek Ashtar University of Technology, Tehran, Iran

ABSTRACT

Keywords: *Vectorized high order expansion, non-linear optimal control, booster landing, optimal guidance*

This study proposes a new non-linear guidance law for a Falcon 9 missile booster landing's terminal phase using a non-linear vectorized high expansion method. For this purpose, At first, the dynamic modeling of the landing problem is presented, assuming mass, gravity, and density are variables. Then, sensitivity variables are extracted using the vectorized high order expansion method and assuming the parameters constant. Then, the guidance law is extracted to update the path and optimal commands using sensitivity variables. The path and commands of the near-optimal guidance are extracted online using the proposed guidance law. Considering initial deviations, the guidance law performance in simulations are studied using a combination of various initial deviations. The results shown as charts and numerical values of errors indicate that the landing point errors are insignificant, and the vectorized high order expansion method has a desirable performance for the reusable booster's vertical landing.

Nomenclature

$f(\dots)$	General Nonlinear Function
g	Gravity Acceleration
g_0	Gravity Acceleration T Zero
h	Height
m	Mass
m_0	Initial Mass
s	Characteristic Area
t	Time
t_f	Terminal Time
u	Optimal Control Command
v	Velocity
v_x	Horizontal Velocity
v_z	Vertical Velocity
x	Range
z	-h
B	Matrix Coefficient of Control Variable
C_{D0}	Base Drag Coefficient
C_{D_α}	Drag Coefficient Derivative
C_{L_α}	Lift Coefficient Derivative
D	Drag
D'	Modified Drag
H	Hamiltonian
I_{sp}	Specific Impulse
J	Performance Index
L	Lift
L'	Modified Lift
R_E	Earth Radius
R_α	Angle of Attack Weigh
$R_{\alpha_{rate}}$	Angle of Attack Rate Weigh
T	Thrust Force

1 PhD. Candidate

2 Associate Professor (Corresponding Author) **Email: rahbar_nas@mut.ac.ir**

3 Assistant Professor

4 Assistant Professor

DOI : 10.22034/jast.2022.327899.1113

Submit: 06.02.2022 / Accepted: 03.04.2022

Print ISSN:1735-2134 Online ISSN: 2345-3648

T_x	Horizontal Thrust Force
T_z	Vertical Thrust Force
	Greek Letters
α	Angle of attack
α_{rate}	Angle of attack rate
γ	Flight Path
δ	Deviation
λ	Costate Variable
ρ	Density
ρ_0	Density at Sea Level

Introduction

Researchers have extensively studied the landing of moon landers and Mars landers until now. They have studied the moon lander's guidance and vertical landing in [1], and the landing of a Mars lander has been studied in [2]. However, thanks to the advent of vertical landing reusable boosters, it has become a popular subject of study. In [3], the authors use particle swarm optimization to design the landing path of the booster with the minimum fuel.

One of the most critical issues in a reusable booster mission is designing and extracting the landing path. One of the popular methods to solve this type of problem is the pseudo-spectral method, which contains a wide range of different primary functions. In another study, [4], this problem is directly solved by the pseudo-spectral method.

Generally, some non-linear methods are known as a high order expansion with a wide variety. For example, we can name the classic perturbation theory, the high order expansion method using differential algebra, the vectorized high order expansion method, or the high order expansion implementation using generator functions.

A detailed discussion on the Hamilton-Jacobi theory and canonical phase space and its properties to formulate the problem and solve it using generating functions has been presented in [5]. The Researchers also put forward a complimentary discussion on generating functions in [6], which is the principal purpose of this method to solve particular dynamic problems.

In this paper, we offer that the initial values of the problem's co-state variables can be extracted based on specific parameters (in parametric form).

In [7], an interesting approach for solving the problem of spacecraft arrangement using generating functions has been proposed. Also, this paper explains the expansion method of non-linear functions around the equilibrium point and specifies that the coefficients of a Taylor series for solving the given problem should be found. The Hamilton-Jacobi equations eventually transforms to some non-homogenous linear differential equations that are easy to solve to obtain the coefficients.

In [8], scientists use the generating functions method to design the state feedback control law with general boundary values. The results show that the cost function can be modeled as a combination of current state variables and boundary values. More details are presented in [9], where they designed the optimal guidance law using generating functions for the orbital meeting of two spacecraft, and the guided one has a continuous thrust. In this study, both Hamiltonian and generating functions are expanded to the desired order in the form of the Taylor series. For dynamic modeling of the equations of motion's rendezvous problem, the authors write this problem relatively and expand it to the desired order by the Taylor series. They modeled these equations in the form of planar maneuver; more details on the expansion method of these equations can be found in [10].

We can find a clear and complete explanation of how to use the generating functions and high order expansion to solve the guidance problem in the optimal control formulations [11]. The main concern of this paper is the guidance of a spacecraft to avoid colliding with another.

In [12], researchers have tried to reformulate the generating functions method for the optimal control problems. They used the Taylor series for the high order expansion method in the form of tensor mathematics. A simple problem is also solved using the proposed method. In 2008 [13], the high order expansion method using differential algebra for solving particular dynamic problems was studied. Differential algebra is a tool by the help of which the algebraic operations on functions occur for the function value at the independent variable's point. We can also include high order derivatives in the equations.

Another method for robust guidance in guiding particular problems based on the differential algebra high order expansion method is also proposed and reviewed [4]. In this method, the general concepts of [13] are in place, and the optimal control problem for generating the guidance command is solved. This time in [15], the authors implement a method similar to the previous references for a few different examples, plus presenting the extraction of the equations governing dynamics of the considered guidance problem. In another study using differential algebra [16], now the problem is modeled by considering constraints on the propulsion force. Another interesting application of the high order expansion method and differential algebra has been given in [17]. This study extracted a solution using the high order expansion for a significant range of conditions and parameters. Since the solution is valid, regardless of numerical values of the initial conditions and parameters, this solution is also reused at the beginning of the new period. Another different application of high order expansion and differential algebra in its computations is discussed in [18]. The spacecraft guidance from the Lagrange point and its collision with the moon to destroy the spacecraft are the main concerns.

Change and deviation in the final time of the problem are probable, which has a deniable effect in solving dynamic equations of the problem. The authors review this point in [19]. A study, [20], shows the benefits of using the differential algebra high order expansion to prevent the collision. This study performs the predictive analysis of deviation from the reference path due to the mentioned deviations for six different objects using the 4th order expansion of differential algebra. Then, the study completes in [21], and the probability of collision using the Monte Carlo analysis is estimated. The Monte Carlo analysis can be estimated using the differential algebra high order expansion. In [22-24], the authors introduce a different approach to the high order expansion named the vectorized high order expansion. The concern of [24] is the maneuver with the help of aerodynamic force considering the optimal guidance. This method does not use differential algebra and implements the mathematical structure required for computations by introducing sensitivity variables and particular algorithms. These sensitivities are computed for both state and co-state variables and are a function of time. As a result, we can obtain the new optimal control command due to any specific initial deviation. Nevertheless, this study aims to review the effectiveness of the high order expansion method and solve the problem of the booster's terminal landing phase of Falcon 9. Due to the ease of implementation, we modeled the problem in planar form to analyze the results and the vectorized high order expansion method performance.

In this study, at first, we define the considered problem and present its mathematical modeling. Then, we provide a brief review of the vectorized high order expansion method. Then, we solve the problem at hand using the vectorized high order expansion method and present the initial results. After that, we explain the implementation results in various simulations and discuss the effectiveness of the vectorized high order expansion method. In the end, we discuss the results and findings of this study.

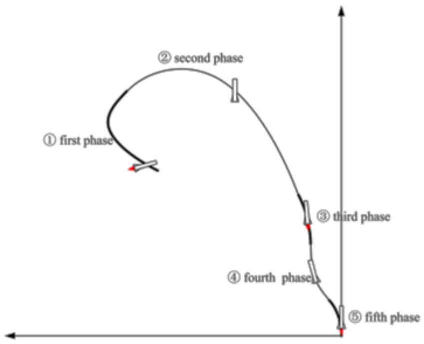

Figure 1: The schematic image of the booster's landing phases [4]

Problem Description

The booster's landing mission includes several phases. We can consider these phases when the engine is either on or off. However, in this study, the authors only consider the terminal phase. In this study, we deal with the booster's terminal landing phase. We assume that in this problem, the booster's engine is always running, and the amount and direction of the propulsion force are controllable. The goal is to satisfy the terminal conditions at the landing point accurately. As a result, the guidance law is modeled in the form of an optimal control problem with bounded terminal conditions.

Mathematical model for simulation

The mathematical model of the dynamic booster is presented as equation 1, assuming point-mass and flat-earth.

$$\begin{aligned}\dot{x} &= v_x\\ \dot{z} &= v_z\\ \dot{v_x} &= -\frac{D}{m}\frac{v_x}{\sqrt{v_x^2+v_z^2}}+\frac{L}{m}\frac{v_z}{\sqrt{v_x^2+v_z^2}}+\frac{T_x}{m}\\ \dot{v_z} &= -\frac{D}{m}\frac{v_z}{\sqrt{v_x^2+v_z^2}}-\frac{L}{m}\frac{v_x}{\sqrt{v_x^2+v_z^2}}+g+\frac{T_z}{m}\\ \dot{\alpha} &= \alpha_{rate}\end{aligned} \quad (1)$$

The dynamic model of the problem is extracted in the earth-fixed reference frame that the center is at the landing point, the first axis is to the right, and the third axis is downward. In this equation, x and z are equal to the range and height, respectively. Similarly, v_x and v_z are horizontal and vertical components of the velocity vector, respectively. Since lift and drag are involved in dynamics, α is considered as the attack angle. Also, T_x are T_z the horizontal and vertical thrust forces and variable rate of attack angle change. The three recent variables are the control variable of the guidance problem. The dynamic modeling of the problem is given in Fig. 1.

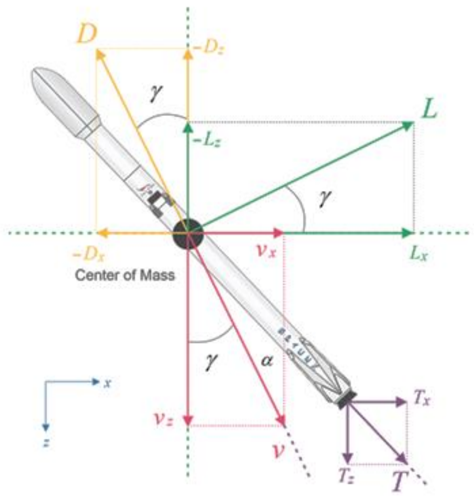

Figure 2: Dynamic Modeling of the Problem

Also, m is the variable time mass of the booster that is modeled by (2):

$$\dot{m} = -\frac{T}{I_{sp}g_0}$$
$$T = \sqrt{T_x^2+T_z^2} \quad (2)$$

where I_{sp} equals 320 represents the particular engine and g_0 equals 9.81. Eventually, in equation (1), L and D are lift and drag forces, respectively, as modeled in equation (3).

$$D = \frac{1}{2}\rho v^2 s(C_{D_0}+C_{D_\alpha}\sin(2\alpha-\frac{\pi}{2}))$$
$$L = \frac{1}{2}\rho v^2 s C_{L_\alpha}\sin 2\alpha \quad (3)$$

where v is computed in the form of equation 4.

$$v = \sqrt{v_x^2+v_z^2} \quad (4)$$

In equation 3, ρ represents the atmosphere density that we calculate using the COESA[1] standard model. It is noteworthy that although the problem's dynamic model is a point-mass model, the state variable is considered for the attack angle, and its change rate is considered a control variable due to the presence of aerodynamic forces. Eventually, in (1), g represents the gravity as shown in (5).

$$g = g_0\left(\frac{R_E}{R_E-z}\right)^2 \quad (5)$$

In this equation, R_E is the earth's radius, which equals 6378 km.

The proposed aerodynamic model is taken from [4], where simulation-related parameters are as follows:

$$\begin{aligned}C_{D_0} &= 9.4\\ C_{D_\alpha} &= 6.5\frac{1}{deg}\\ C_{L_\alpha} &= 4\ \frac{1}{deg}\\ s &= 10.752\ m^2\end{aligned} \quad (6)$$

Mathematical model for solving the landing problem

In what follows, we use equations (1-6) to implement landing simulations. However, we benefitted from the following assumptions to extract the path and guidance law:

1- Gravity is constant and equals $g = g_0$
2- Density is constant, equals to $\rho = \rho_0$ and 1.225
3- Mass is constant and equals $m = m_0$

As a result, the dynamic equations in (1) will be used as the reference model for solving the landing problem, while $T_x' = \frac{T_x}{m_0}$ and $T_z' = \frac{T_z}{m_0}$. In addition, variables D' and L' are defined as (7); however, the aerodynamic parameters are as (6) same as before.

$$D' = \frac{\frac{1}{2}\rho_0 v^2 s}{m_0}\left(C_{D_0} + C_{D_\alpha}\sin(2\alpha - \frac{\pi}{2})\right) \\ L' = \frac{\frac{1}{2}\rho_0 v^2 s}{m_0} C_{L_\alpha}\sin 2\alpha \tag{7}$$

Now the cost function is expressed as (8) to implement the model proposed in (1) and (7) in the optimal control theory:

$$\begin{cases} J = \frac{1}{2}\int_0^{t_f}\left(T_x'^2 + T_z'^2 + R_\alpha \alpha^2 + R_{\alpha_{rate}}\alpha_{rate}^2\right)dt \\ R_{\alpha_{rate}} = 7.5\left(\frac{180}{\pi}\right)^2 \\ R_\alpha = 0.03\left(\frac{180}{\pi}\right)^2 \end{cases} \tag{8}$$

Where t_f is the terminal time. Eventually, the initial and final conditions should be determined to solve this problem. These parameters are expressed in (9):

$$\begin{gathered} x_i = 1000\,m, \quad x_f = 0\,m \\ z_i = -4400\,m, \quad z_f = -1\,m \\ v_{x_i} = -136.81\frac{m}{s}, \quad v_{x_f} = 0\frac{m}{s} \\ v_{z_i} = 375.88\frac{m}{s}, \quad v_{z_f} = 0.25\frac{m}{s} \\ \alpha_i = 0\,rad, \quad \alpha_f = 0\,rad, m_0 = 4.7e+4\,kg \end{gathered} \tag{9}$$

These parameters are selected relatively similar to the study [4]. In the above equation, subscript i represents initial conditions and f represents final conditions. Therefore, we can use the parameters of (10), which represent the initial and the final nominal values of the state variables, to solve the optimal control problem for extracting the reference solution. In the next section, we briefly review the high order expansion method, which is the principal tool for solving the problem in this study.

A Review of the High Order Expansion Method

In this section, we have tried to express the general concept and the procedure of the high order expansion method. Moreover, we describe concepts like sensitivities and the method of determining their initial values. To clarify the method implementation, we assume that the considered problem is defined as a non-linear univariate one. Assume that equation (10) represents the dynamic equation of a system. This differential equation is non-linear to the state variable but linear to the control input.

$$\dot{x} = f(x) + Bu \tag{10}$$

This dynamic has two goals:
For the given $x(0) = x_0$, by $J = \frac{1}{2}\int_0^{t_f}(qx^2 + ru^2)dt$, by definition, the optimal control, u^*, should be determined so that the state variable is placed on point $x(t_f) = x_f$ at moment t_f. The final conditions' constraint is hard. Suppose we assume that initial conditions have a deviation of δx_0 from x_0. In that case, we should provide a strategy through which $u^*$is updated in the way that in t_f value of δx_f, the deviation from x_f at the final moment equals zero.
Considering the given cost function and according to the optimal control theory:

$$\begin{cases} \dot{\lambda} = -\frac{\partial H}{\partial x} \\ \frac{\partial H}{\partial u} = 0 \rightarrow u = -\frac{B}{r}\lambda \end{cases} \rightarrow \begin{cases} \dot{x} = f(x) - \frac{B^2}{r}\lambda \\ \dot{\lambda} = -qx - \frac{\partial f}{\partial x}\lambda \end{cases} \tag{11}$$

Where $x(t_0) = x_0$ and $x(t_f) = x_f$ are desirable for the above differential equation system as per the definition. The above differential equation system is a problem with distinct boundary values. However, we can solve an initial value problem in the form of a leading integration. Now, deviation in the initial conditions of the problem is considered according to Fig. 3; initial conditions deviation from the nominal value in real problems is always probable due to turbulence and uncertainty. Therefore, if the initial conditions at the time of guidance law implementation, i.e., implementing a real problem or simulation, are different from the nominal value, performing the open-loop optimal control command which was obtained in the previous stage, will lead to enormous deviations in final conditions.

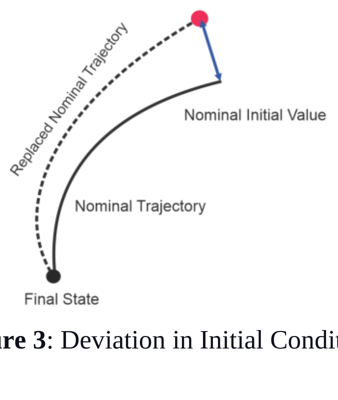

Figure 3: Deviation in Initial Conditions

Assuming that the problem deviates from the initial conditions, this would be a new optimal control problem. However, we should be aware that resolving the optimal control problem should be online. Using numerical methods such as the spectral method is not efficient from the point of time and cost. The better solution is to find a new optimal path (and optimal control) and substitute it with the previous optimal path (and optimal control).

Replacing the nominal path using the high order expansion method has an offline computational load. However, once calculating the coefficients, we can use it in an online form and replace the optimal control command and optimal path according to the initial deviation value. In (11), since $x_n = x^*$ and $\lambda_n = \lambda^*$ are extracted from these equations using the numerical method, the solution applies to the above equation. So,

$$\begin{cases} \dot{x}^* = f(x^*) - \dfrac{B^2}{r}\lambda^* \\ \dot{\lambda}^* = -qx^* - \dfrac{\partial f}{\partial x}\lambda^* \end{cases} \tag{12}$$

Now, if there is a deviation in initial conditions, i.e., $x(0) = x_0 + \delta x_0$, x_n and λ_n should be substituted by the values of (13):

$$\begin{cases} x^* = x_n + \delta x \\ \lambda^* = \lambda_n + \delta\lambda \end{cases} \tag{13}$$

then, the result is:

$$\begin{cases} \dot{x_n} + \dot{\delta x} = f(x_n + \delta x) - \dfrac{B^2}{r}(\lambda_n + \delta\lambda) \\ \dot{\lambda_n} + \dot{\delta\lambda} = \\ -q \times (x_n + \delta x) - \dfrac{\partial f}{\partial x} \times (\lambda_n + \delta\lambda) \end{cases} \tag{14}$$

In the next step, we estimate function $f(x)$ with its Taylor series around the nominal path because equations and their solving process for non-linear functions will be generalized. We can expand this Taylor series to the desired N^{th} order; however, here, we only expand to the 2^{nd} order to avoid complexity.

$$\begin{cases} \dot{x} + \dot{\delta x} = \\ \{f(x_n) + c_1\delta x + c_2\delta x^2 + \cdots\} \\ -\dfrac{B^2}{r}(\lambda_n + \delta\lambda) \\ \dot{\lambda_n} + \dot{\delta\lambda} = -q(x_n + \delta x) \\ -\dfrac{\partial}{\partial x}\{f(x_n) + c_1\delta x + c_2\delta x^2 + \cdots\} \\ \times (\lambda_n + \delta\lambda) \end{cases} \tag{15}$$

In this equation, $c_1 = \frac{\partial f}{\partial x_n}$ and $c_2 = \frac{1}{2}\frac{\partial^2 f}{\partial x_n^2}$ are the Taylor series coefficients, and since they are calculated on the nominal path, they are a function of time. In the following solution step, we subtract the nominal solution from the two sides of the equation. The result is:

$$\begin{cases} \dot{\delta x} = c_1\delta x + c_2\delta x^2 + \cdots - \dfrac{B^2}{r}\delta\lambda \\ \dot{\delta\lambda} = -q\delta x - (c_1\delta\lambda + 2c_2\delta x\delta\lambda + \cdots) \end{cases} \tag{16}$$

Now, we assume that this value equals a fixed unknown value of α that is $\alpha = \delta x_0$. Then we assume that deviations are defined as a function of α.

$$\delta x(t) = {}_x^1s(t) \times \alpha + {}_x^2s(t) \times \alpha^2 + \cdots \tag{17}$$

In (17), ${}_x^1s(t)$ and ${}_x^2s(t)$ are the first and the second-order sensitivity of the state variable to the deviation in the initial conditions, respectively, showing the effect of initial deviations on the future optimal control problem where the sensitivities are unknown. Another equation is similarly defined for $\delta\lambda$.

$$\delta\lambda(t) = {}_\lambda^1s(t) \times \alpha + {}_\lambda^2s(t) \times \alpha^2 + \cdots \tag{18}$$

Now, we can put the two defined equations and the differential equations of the deviational variables together and conclude:

$$\begin{cases} \dot{\delta x} = c_1\delta x + c_2\delta x^2 + \cdots - \dfrac{B^2}{r}\delta\lambda \\ \dot{\delta\lambda} = -q\delta x - (c_1\delta\lambda + 2c_2\delta x\delta\lambda + \cdots) \\ \delta x(t) = {}_x^1s(t) \times \alpha + {}_x^2s(t) \times \alpha^2 + \cdots \\ \delta\lambda(t) = {}_\lambda^1s(t) \times \alpha + {}_\lambda^2s(t) \times \alpha^2 + \cdots \end{cases} \tag{19}$$

In the next step, by reviewing the above equation, we can substitute the two following equations in the two above differential equations:

$$\begin{cases} \dfrac{d}{dt}({}_x^1s(t)\alpha + {}_x^2s(t)\alpha^2) = \\ c_1({}_x^1s(t)\alpha + {}_x^2s(t)\alpha^2) \\ +c_2({}_x^1s(t)\alpha + {}_x^2s(t)\alpha^2)^2 \\ -\dfrac{B^2}{r}({}_\lambda^1s(t)\alpha + {}_\lambda^2s(t)\alpha^2) \\ \dfrac{d}{dt}({}_\lambda^1s(t)\alpha + {}_\lambda^2s(t)\alpha^2) = \\ -c_1({}_\lambda^1s(t)\alpha + {}_\lambda^2s(t)\alpha^2) \\ -2c_2({}_x^1s(t)\alpha + {}_x^2s(t)\alpha^2) \\ \times ({}_\lambda^1s(t)\alpha + {}_\lambda^2s(t)\alpha^2) \end{cases} \tag{20}$$

As a result:

$$\begin{cases} {}^{1}_{x}\dot{s}(t) = c_1 {}^{1}_{x}s(t) - \dfrac{B^2}{r}\,{}^{1}_{\lambda}s(t) \\ {}^{1}_{\lambda}\dot{s}(t) = -q\,{}^{1}_{x}s(t) + c_1\,{}^{1}_{\lambda}s(t) \\ {}^{2}_{x}\dot{s}(t) = c_1\,{}^{2}_{x}s(t) - \dfrac{B^2}{r}\,{}^{2}_{\lambda}s(t) + c_2\,{}^{1}_{x}s(t)^2 \\ {}^{2}_{\lambda}\dot{s}(t) = -q\,{}^{2}_{x}s(t) - c_1\,{}^{2}_{\lambda}s(t) - 2c_2\,{}^{1}_{x}s(t)\,{}^{1}_{\lambda}s(t) \end{cases} \tag{21}$$

The remarkable feature of the differential equations in equation (21) for sensitivities is that they are all linear and time-variable. However, except for the first-order sensitivities, the other sensitivities have a non-homogenous equation system, where non-homogenous expressions are calculated according to lower-order sensitivities. As a result, we can perform the extraction of sensitivities from the first order to the N[th] step by step, and for this, we solve a time-variable linear differential equation system in each step.

Now that we extracted the sensitivities, we can see by referring to (17) and (18) that expressions $\delta x(t)$ and $\delta\lambda(t)$ are calculated, and the result is:

$$\begin{cases} x_n^{new}(t) = x_n^{old}(t) + \delta x(t) \\ \lambda_n^{new}(t) = \lambda_n^{old}(t) + \delta\lambda(t) \end{cases} \tag{22}$$

, which expresses that we can extract the new nominal solution by adding the calculated values of deviational variables to the initial nominal solution. Therefore, since λ_n^{new} is extracted, the new nominal optimal control command will be obtained by using $u_n^{new} = -\frac{B}{r}\lambda_n^{new}$. For more details on implementing the multi-variable vectorized high order expansion method, we may refer to [22-24].

Using the High Order Expansion Method

Now that we reviewed the vectorized high order expansion method and its application in the optimal control problem solving, we present the initial results of the landing problem solving with the help of the method in this section. At First, we extract the nominal solution of the landing problem using the numerical method considering equation (1), (7), and (8) and the initial and the final conditions provided in (9). To extract the final time, we considered this as an optimization parameter, thus obtaining 30/7105 seconds for the nominal value of the final time t_f. Then, sensitivities for this model are extracted to the third order. Now, according to:

$$\begin{aligned} \frac{\partial\mathcal{H}}{\partial T'_x} = 0 &\rightarrow T'_x = -\lambda_3 \\ \frac{\partial\mathcal{H}}{\partial T'_z} = 0 &\rightarrow T'_z = -\lambda_4 \\ \frac{\partial\mathcal{H}}{\partial \alpha_{rate}} = 0 &\rightarrow \alpha_{rate} = -\frac{\lambda_5}{R_{\alpha_{rate}}} \end{aligned} \tag{23}$$

We can extract the optimal commands. To do this, having $\boldsymbol{\delta} s_0 = \begin{bmatrix}\delta x_0 & \delta z_0 & \delta v_{x_0} & \delta v_{z_0} & \delta\alpha_0\end{bmatrix}^T$, we can calculate the values of δx ، δz ، δv_x ، δv_z, and $\delta\alpha$, and also $\delta\lambda_3$ ، $\delta\lambda_4$, and $\delta\lambda_5$ for all flight moments. Then, considering:

$$\begin{aligned} x_r &= x_n + \delta x \\ z_r &= z_n + \delta z \\ v_{x_r} &= v_{x_n} + \delta v_x \\ v_{z_r} &= v_{z_n} + \delta v_z \\ \alpha_r &= \alpha_n + \delta\alpha \end{aligned} \tag{24}$$

and

$$\begin{aligned} T'_x &= -(\lambda_{3_n} + \delta\lambda_3) \\ T'_z &= -(\lambda_{4_n} + \delta\lambda_4) \\ \alpha_{rate} &= -\frac{(\lambda_{5_n} + \delta\lambda_5)}{R_{\alpha_{rate}}} \end{aligned} \tag{25}$$

, we calculate the reference path and guidance commands according to the initial deviation. In (24) and (25), subscripts r and n for state and co-state variables represent the reference solution and the nominal solution, respectively. Now we evaluate the performance of the high order expansion method by considering different initial deviations for condition and velocity. The vectorized high order expansion method diagram block is shown in Fig. 4.

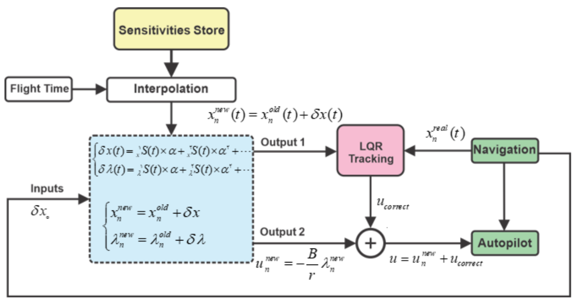

Figure 4: The guidance diagram block using the vectorized high order expansion method

In this block-diagram, first, the relevant sensitivities are extracted. Then, the optimal guidance command through (19) and (20) and also $\delta x(t)$ and $\delta\lambda(t)$ are extracted considering the initial deviation by means of interpolation of sensitivities. Then, the $\delta x(t)$ obtained from the block of sensitivities is compared with the actual $\delta x(t)$ obtained from the navigation sensors. If there is a deviation, the correction command is produced using an LQ regulator and is added to the guidance command obtained from the block of sensitivities. Then, again it is transmitted to the autopilot to correct the path in case of any deviation.

Overall, eight different simulations are performed according to the equations of (7). Table 1 shows these eight different modes.

Table 1: Considering different initial deviations for condition and velocity

S.N.	$\delta v_{z_0}[\frac{m}{s}]$	$\delta v_{x_0}[\frac{m}{s}]$	$\delta h_0[m]$	$\delta x_0[m]$
1	0	0	0	500
2	0	0	0	-500
3	0	0	300	0
4	0	0	-300	0
5	0	30	0	0
6	0	-30	0	0
7	30	0	0	0
8	-30	0	0	0

Considering that the vectorized high order expansion method is an approximate method, we also benefitted from an LQ tracker of the nominal path to ensure the execution of guidance commands and the precise satisfaction of the final conditions. The results of these eight simulations at the final point are shown in Table 2.

Table 2: Simulation results

	$t_f[s]$	α_f [$^\circ$]	$v_{z_f}[\frac{m}{s}]$	$v_{x_f}[\frac{m}{s}]$	x_f $[m]$
1	30.711	-0.0016	0.2624	-0.0026	0.0119
2	30.712	-0.00052	0.2661	-0.0018	0.0064
3	30.710	0.00043	0.2506	-0.0008	0.0026
4	30.710	-0.00075	0.2505	-0.00082	0.0021
5	30.710	-0.00007	0.2506	-0.00007	0.0003
6	30.710	-0.00003	0.25	-0.00002	0.00003
7	30.710	-0.000004	0.2503	0.000007	0.0001
8	30.7105	0.000005	0.2504	0.00002	-0.0002

In simulations, the criterion for a stop is reaching the height of 1 meter. It should be noted that $h = -z$ and $\delta h_0 = -\delta z_0$. We can observe that the average error equals 0.0029, and its standard deviation equals 0.0042. The average value and standard deviation for error v_{x_f} are 0.0035 and 0.0062, respectively. For error α_f, the average value is equal to -3.17e-4 and the standard deviation is equal to 6.3e-4. The final time error equals 3.5e-4 and 0.9e-4. Diagrams of the trajectory and acceleration commands in two directions for the first four simulations are shown in Fig. 4-6.

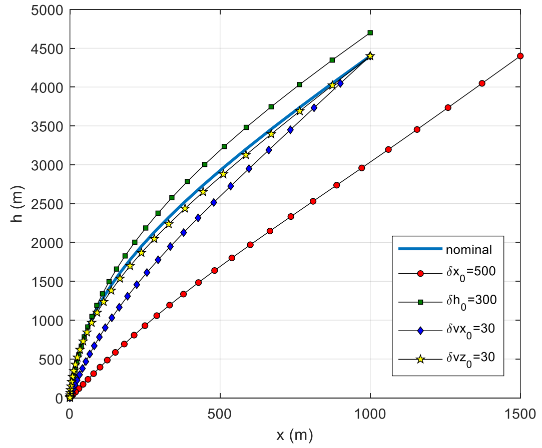

Figure 5: trajectory

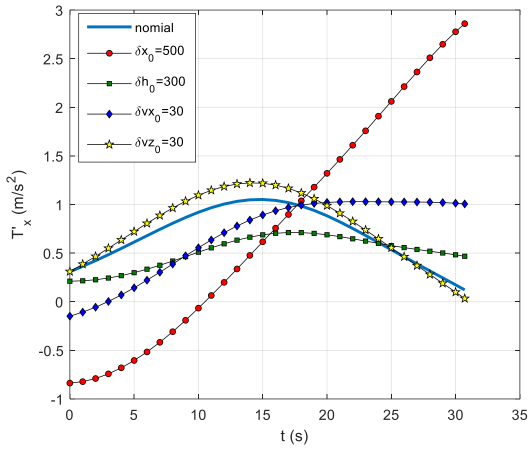

Figure 6: Horizontal acceleration command

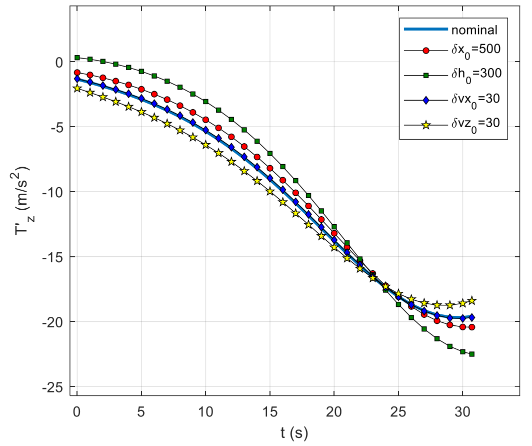

Figure 7: Vertical acceleration command

As seen, errors are insignificant in the performed simulations, and the final conditions and the final time are provided with high accuracy. Errors are minimal in these simulations and arise from the fact that the vectorized high order expansion method solution is an approximate method. However, the results will be more challenging by including the mass model, density, and gravity in the simulations, which will be explained in the next section.

The Analysis of the Simulation Results

Some simplifications, including constant mass, constant density, and constant gravity in dynamic equations, were considered to solve the vectorized high order expansion for the landing problem. The high order expansion solution's performance in some simulations was reviewed in section 4 by maintaining the assumptions. However, to better investigate and evaluate the performance, we review the effect of these variables. Note that the perfect gravity model is used in all simulations of this section. Therefore, height deviations are considered from -300 m to 300 m with 100 m steps, range deviations from -500 m to 500 m with 100 m steps, and horizontal and vertical velocity deviations from -30 m/s to 30 m/s with 10 m steps. All its various combinations are simulated separately for deviations of condition and velocity. In the continuation of this section, first, the variable mass effect is considered, and then, the variable density effect is considered (the variable gravity model is used in both conditions) to study the effectiveness of the high order expansion method and the landing point error for deviations. This error is calculated according to equation 26.

$$MSE = \frac{1}{4}\left\{\frac{\left(x(t_f)-x_f\right)^2}{500} + \frac{\left(z(t_f)-z_f\right)^2}{300} + \frac{\left(v_x(t_f)-v_{x_f}\right)^2}{30} + \frac{\left(v_z(t_f)-v_{z_f}\right)^2}{30}\right\} \tag{26}$$

Studying the Effect of Mass Changes

The effect of variable mass is considered according to equation (2) for simulations, but the density is assumed to be constant and equal to $\rho = \rho_0 = 1.225$. Now, considering the mathematical model, simulations will be performed for the range of initial deviations. Fig. 8 and 9 indicate the contour of landing point error for of the position and the velocity initial deviations, respectively. Also, Table 3 shows the average value and standard deviation of the errors at the landing point. All combinations of the initial deviations of position and velocity are considered to calculate the average value and standard deviation, including 3773 different simulations with different initial deviations. Studying Fig. 8-10 and considering the results in Table 3, we see that the landing point errors are insignificant and are desirable for the booster's landing mission. It should be noted that the height error is zero because the condition considered for the termination of simulations to reach the height of 1 meter.

Table 3: The average value and standard deviation of the landing point error

	$x(t_f) - x_f$	$v_x(t_f) - v_{x_f}$	$v_z(t_f) - v_{z_f}$
Mean	0.0745	-0.0267	0.07611
Standard Deviation	0.0933	0.0192	0.1297

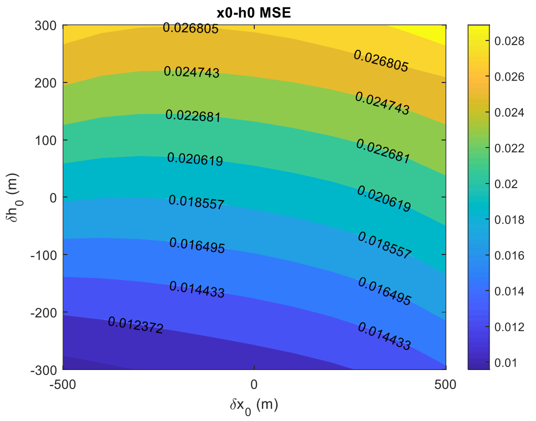

Figure 8: The error contour at the landing point caused by the initial deviation of position

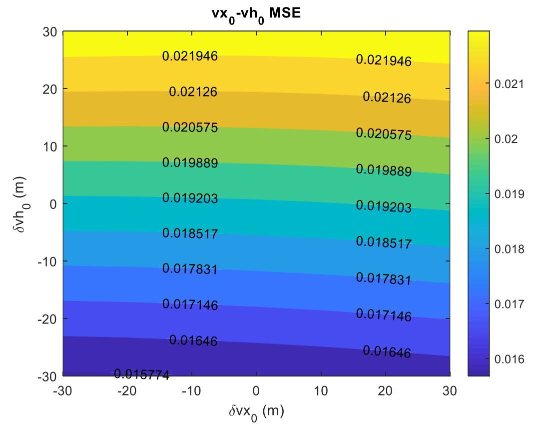

Figure 9: The error contour at the landing point caused by the initial deviation of velocity

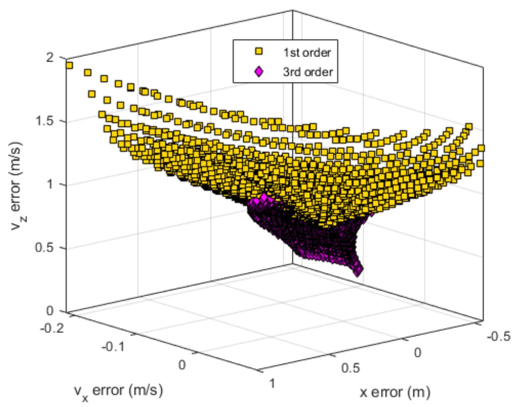

Figure 10: Distribution of range error and horizontal and vertical velocity comparing the first order and the third order solutions

Studying the Effects of Density Changes

Similarly, we consider the previous simulations this time using the variable density but with constant mass. Fig. 11-13 illustrate the simulation results. In the same way, the average value and the standard deviation of the landing point errors for all different combinations of the initial deviations are shown in Table 4. It is seen from Table 4 that the initial deviation in velocity has a more negligible effect on the vertical velocity at the landing point compared to the initial deviation of position, while its effect on the horizontal velocity error and horizontal distance is far more. However, the error values are still small, and the implemented guidance method shows good quality.

Table 4: The average value and standard deviation of the landing point

	$x(t_f) - x_f$	$v_x(t_f) - v_{x_f}$	$v_z(t_f) - v_{z_f}$
Mean	0.1171	-0.0435	0.0909
Standard Deviation	0.0351	0.0279	0.0244

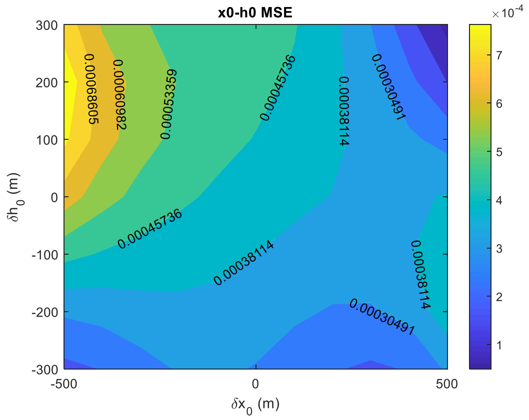

Figure 11: The error contour at the landing point caused by the initial deviation of position

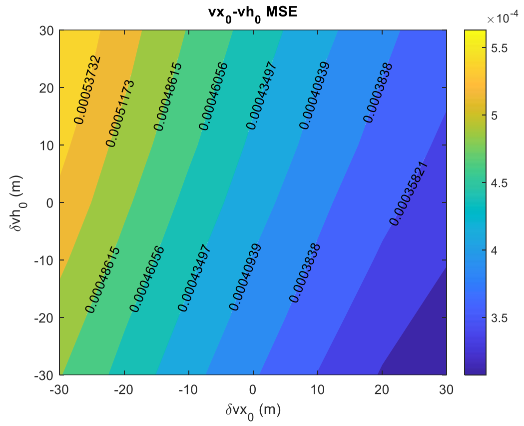

Figure 12: The error contour at the landing point caused by the initial deviation of velocity

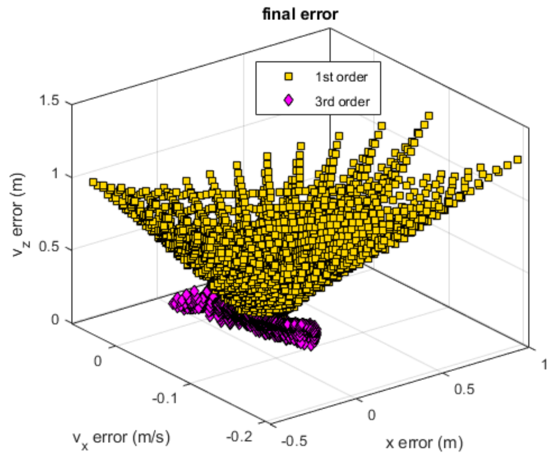

Figure 13: Range error distribution and horizontal and vertical velocity comparing the first and the third-order solution

Conclusion and Final Words

In this study, we considered the terminal phase landing of a typical booster, while the principal purpose was to provide the least possible errors at the landing point. Therefore, we first presented a dynamic modeling for implementing simulations, and subsequently, a simpler dynamic model to solve the optimal control problem using the vectorized high order expansion method. Therefore, in what followed, we provided a brief review of the vectorized high order expansion method and its implementation in the optimal control problem. Then, we solved the booster landing problem up to the third order. We presented eight simulations with different initial deviations to study the theoretical errors. Later, we considered more comprehensive simulations to estimate the quality of the high order method in the presence of uncertainties and to evaluate the effect of higher-order expressions. Although we considered mass, density, and gravity to be constant in the mathematical model to extract the solution using the high order expansion method, the simulations implemented by considering variable gravity, density, and mass indicated the high quality of the high order expansion method.

References

[1] A. Banerjee and R. Padhi, "An optimal explicit guidance algorithm for terminal descent phase of lunar soft landing," *AIAA Guid. Navig. Control Conf. 2017*, no. January, pp. 1–12, 2017, doi: 10.2514/6.2017-1266.

[2] S. Swaminathan, U. P. Rajeev, and D. Ghose, "Real time powered descent guidance algorithm for mars pinpoint landing with inequality constraints," *AIAA Scitech 2020 Forum*, vol. 1 PartF, no. January, pp. 1–21, 2020, doi: 10.2514/6.2020-1351.

[3] K. S. G. Anglim, Z. Zhang, and Q. Gao, "Minimum - Fuel Optimal Trajectory for Reusable First - Stage Rocket Landing Using Particle Swarm Optimization," *Int. J. Mech. Mechatronics Eng.*, vol. 11, no. 5, pp. 981–990, 2017.

[4] Y. Li, W. Chen, H. Zhou, and L. Yang, "Conjugate gradient method with pseudospectral collocation scheme for optimal rocket landing guidance," *Aerosp. Sci. Technol.*, vol. 104, p. 105999, 2020, doi: 10.1016/j.ast.2020.105999.

[5] V. M. Guibout and D. J. Scheeres, "Solving two-point boundary value problems using generating functions: Theory and Applications to optimal control and the study of Hamiltonian dynamical systems," no. December, 2003, [Online]. Available: http://arxiv.org/abs/math/0310475.

[6] V. M. Guibout and D. J. Scheeres, "Solving Two-Point Boundary Value Problems Using Generating Functions: Theory and Applications to Astrodynamics," *Elsevier Astrodyn. Ser.*, vol. 1, pp. 53–105, 2006, doi: 10.1016/S1874-9305(07)80005-7.

[7] V. M. Guibout and D. J. Scheeres, "Solving relative two-point boundary value problems: Spacecraft formation flight transfers application," *J. Guid. Control. Dyn.*, vol. 27, no. 4, pp. 693–704, 2004, doi: 10.2514/1.11164.

[8] C. Park and D. J. Scheeres, "Determination of optimal feedback terminal controllers for general boundary conditions using generating functions," *Automatica*, vol. 42, no. 5, pp. 869–875, 2006, doi: 10.1016/j.automatica.2006.01.015.

[9] C. Park, V. Guibout, and D. J. Scheeres, "Solving Optimal Continuous Thrust Rendezvous Problems with Generating Functions," *J. Guid. Control. Dyn.*, vol. 29, no. 2, pp. 321–331, Mar. 2006, doi: 10.2514/1.14580.

[10] H. D. Curtis, Orbital Mechanics for Engineering Students. Elsevier, 2013.

[11] K. Lee, C. Park, and S. Y. Park, "Near-optimal continuous control for spacecraft collision avoidance maneuvers via generating functions," Aerosp. Sci. Technol., vol. 62, pp. 65–74, 2017, doi: 10.1016/j.ast.2016.11.026.

[12] Z. Hao, K. Fujimoto, and Q. Zhang, "Approximate Solutions to the Hamilton-Jacobi Equations for Generating Functions," J. Syst. Sci. Complex., vol. 33, no. 2, pp. 261–288, 2020, doi: 10.1007/s11424-019-8334-6.

[13] P. Di Lizia, R. Armellin, and M. Lavagna, "Application of high order expansions of two-point boundary value problems to astrodynamics," *Celest. Mech. Dyn. Astron.*, vol. 102, no. 4, pp. 355–375, 2008, doi: 10.1007/s10569-008-9170-5.

[14] P. Di Lizia, R. Armellin, A. Ercoli-Finzi, and M. Berz, "High-order robust guidance of interplanetary trajectories based on differential algebra," *J. Aerosp. Eng. Sci. Appl.*, vol. 1, no. 1, pp. 43–57, Jan. 2008, doi: 10.7446/jaesa.0101.05.

[15] P. Di Lizia, R. Armellin, F. Bernelli-Zazzera, and M. Berz, "High order optimal control of space trajectories with uncertain boundary conditions," *Acta Astronaut.*, vol. 93, pp. 217–229, 2014, doi: 10.1016/j.actaastro.2013.07.007.

[16] P. Di Lizia, R. Armellin, A. Morselli, and F. Bernelli-Zazzera, "High order optimal feedback control of space trajectories with bounded control," *Acta Astronaut.*, vol. 94, no. 1, pp. 383–394, 2014, doi: 10.1016/j.actaastro.2013.02.011.

[17] A. Wittig and R. Armellin, "High order transfer maps for perturbed Keplerian motion," *Celest. Mech. Dyn. Astron.*, vol. 122, no. 4, pp. 333–358, 2015, doi: 10.1007/s10569-015-9621-8.

[18] M. Vetrisano and M. Vasile, "Analysis of spacecraft disposal solutions from LPO to the Moon with high order polynomial expansions," *Adv. Sp. Res.*, vol. 60, no. 1, pp. 38–56, 2017, doi: 10.1016/j.asr.2017.04.005.

[19] Z. J. Sun, P. Di Lizia, F. Bernelli-Zazzera, Y. Z. Luo, and K. P. Lin, "High-order state transition polynomial with time expansion based on differential algebra," *Acta Astronaut.*, vol. 163, no. July 2018, pp. 45–55, 2019, doi: 10.1016/j.actaastro.2019.03.068.

[20] A. Morselli, R. Armellin, P. Di Lizia, and F. Bernelli Zazzera, "A high order method for orbital conjunctions analysis: Sensitivity to initial uncertainties," *Adv. Sp. Res.*, vol. 53, no. 3, pp. 490–508, 2014, doi: 10.1016/j.asr.2013.11.038.

[21] A. Morselli, R. Armellin, P. Di Lizia, and F. Bernelli Zazzera, "A high order method for orbital conjunctions analysis: Monte Carlo collision probability computation," *Adv. Sp. Res.*, vol. 55, no. 1, pp. 311–333, 2015, doi: 10.1016/j.asr.2014.09.003.

[22] M. Moghadasian and J. Roshanian, "Optimal Landing of Unmanned Aerial Vehicle Using Vectorised High Order Expansions Method",*Modares Mechanical Engineering*

vol. 19, no. 11, pp. 2761–2769, 2019, [Online]. Available: http://mme.modares.ac.ir/article-15-27084-en.html.

[23] M. Moghadasian and J. Roshanian, "Continuous maneuver of unmanned aerial vehicle using High Order Expansions method for optimal control problem," *Modares Mechanical Engineering* vol. 17, no. 12, pp. 382–390, 2018, [Online]. Available: http://mme.modares.ac.ir/article-15-4456-en.html.

[24] M. Moghadasian and J. Roshanian, "Approximately optimal manoeuvre strategy for aero-assisted space mission," *Adv. Sp. Res.*, vol. 64, no. 2, pp. 436–450, 2019, doi: 10.1016/j.asr.2019.04.003.